Promotion of cooperation in deme-structured populations with growth-merging dynamics

Damien Ribière, Alia Abbara,* and Anne-Florence Bitbol†
Institute of Bioengineering, School of Life Sciences, École Polytechnique Fédérale de Lausanne (EPFL), CH-1015 Lausanne, Switzerland
and SIB Swiss Institute of Bioinformatics, CH-1015 Lausanne, Switzerland

(Received 25 January 2026; accepted 14 October 2026; published 9 November 2026)

The spatial structure of populations may promote the emergence and maintenance of cooperation. Cooperation in the prisoner's dilemma is favored under specific update rules in evolutionary graph theory models with one individual per node of a graph, but this effect vanishes in models with well-mixed demes connected by migrations under soft selection (each deme contributing independently of its productivity). In contrast, experiments and models involving cycles of growth, merging and dilution have shown that spatial structure can favor cooperation. Here, we reconcile these findings by studying deme-structured populations under growth-merging-dilution dynamics, corresponding to a clique (fully connected graph) under hard selection (each deme contributing in proportion to its productivity). We obtain analytical conditions for the cooperator fraction to increase during deterministic logistic growth, and to increase on average under dilution-growth-merging cycles, in the weak selection regime, where fitness differences between genotypes are small. Furthermore, we analytically express the fixation probability of cooperators under weak selection, yielding a criterion for cooperators to have a higher fixation probability than neutral mutants. Finally, numerical simulations show that stochastic growth further promotes cooperation. Overall, hard selection is essential for cooperation to be promoted in deme-structured populations.

DOI: 10.1103/wlyc-rtgs

I. INTRODUCTION

Understanding the emergence and maintenance of cooperation is an important question in biology. As cooperative behavior benefits other individuals but entails a cost for the cooperator individual, noncooperators tend to be advantaged by natural selection. Nevertheless, cooperation is often observed in nature, from microorganisms to animals [1–5]. This apparent paradox is known as the dilemma of cooperation [6]. In particular, bacteria interact by secreting various molecules, some of which are public goods, i.e., shared resources that bring a metabolic cost for the producers, but benefit all other bacteria in the population, including nonproducers (cheaters) [6,7]. Different mechanisms may explain the evolution of cooperation under some conditions. One of them is kin selection [8–11]: if individuals that are genetically related to cooperators benefit most from cooperation, then it can be selected despite its cost. Another one is spatial structure, which has been investigated theoretically [6,12–19] and experimentally [20–22]. Since genetically related individuals are often closely located in spatially structured populations, the ability of spatial structure to enhance cooperation is related to kin selection [23].

In evolutionary graph theory, a simple and minimal model of cooperation in spatially structured populations is the prisoner's dilemma game [24–26], played on graphs with one individual per node [27]. It was shown that cooperation can be favored by natural selection in the prisoner's dilemma game in some graph structures [12,13]: a cooperator is then more likely to take over the structured population than a neutral mutant. However, these results strongly depend on the update rule that specifies how individuals divide, die, and replace each other (e.g., death-birth or birth-death). Recently, we developed general models of structured populations [28,29], where each node of the graph comprises a well-mixed deme (i.e., subpopulation) instead of a single individual. Our models do not involve choosing an individual-level update rule connecting the birth, death, and migration events of individuals, which impacts fixation probabilities [30–32]. Such a level of description is difficult to justify for microbes, unlike deme-level protocols that can be set experimentally [33]. The deme-level demographic scheme nonetheless shapes evolutionary outcomes, as we show here. In Ref. [34], we studied the evolution of cooperation in these models under soft selection, namely, when each deme contributes a number of individuals independent of its composition. We showed that cooperation is not favored by spatial structure in this case: a cooperator is less likely to take over the structured population than a neutral mutant [34]. However, previous studies that considered populations

*Present address: Sorbonne Université, CNRS, Institut de Biologie Paris-Seine (IBPS), Laboratoire Jean Perrin (LJP), Paris, France.
†Contact author: anne-florence.bitbol@epfl.ch

Published by the American Physical Society under the terms of the Creative Commons Attribution 4.0 International license. Further distribution of this work must maintain attribution to the author(s) and the published article's title, journal citation, and DOI.

undergoing cycles of growth in subpopulations, merging of all subpopulations, and bottlenecks yielding new subpopulations demonstrated that the total fraction of cooperators can increase in time [6,14–17,20–22]. This occurs due to Simpson's paradox [20]: if there is sufficient heterogeneity of composition between subpopulations, the fraction of cooperators can increase overall, despite its decrease in each separate subpopulation, which results from the individual cost of cooperation, because subpopulations with more cooperators grow faster than others.

Here, we reconcile the results of Ref. [34] with those of Refs. [6,14–17,20–22]. As in Ref. [34], we use our general model of structured populations [29], which accounts for cycles of growth and dilution-migration, and we consider individuals that interact via a prisoner's dilemma game played in each deme of a structured population. However, we consider that all demes are merged before a new bottleneck state is formed for each deme by sampling from the merged population, as in Refs. [16,17]. Since demes contribute to the next bottleneck state proportionally to their grown sizes, this model implements a simple case of hard selection, where each deme contributes a number of individuals proportional to its productivity [35–37]. Given the symmetry between all demes, this structured population can be viewed as a clique graph (or fully connected graph) with hard selection. This stands in contrast with Ref. [34], where soft selection was assumed.

We analytically determine the time evolution of the cooperator fraction during a deterministic logistic growth phase, in the weak selection regime, where the fitness differences between genotypes are small (a distinct notion from the hard versus soft distinction above, which regards how demes contribute). We interpret our result as a multilevel Price equation [38,39], featuring a trade-off between within-deme dynamics, where cooperators are disadvantaged, and between-deme dynamics, where demes with more cooperators are advantaged. We determine a criterion for the cooperator fraction to increase during the growth phase. Next, we analytically express the expectation value of the variation of the overall cooperator fraction in the structured population, over a full cycle of dilution-growth-merging under weak selection. This allows us to define an effective fitness parameter that determines whether the overall cooperator fraction is expected to grow on average over the dilution-growth-merging dynamics. An important condition for this to happen is that deme bottleneck sizes should be small enough. Then, we analytically determine the fixation probability of cooperators, assuming weak selection but without assuming large demes. We obtain a condition for the fixation of a cooperator to be more favorable than that of a neutral mutant. Finally, using numerical simulations, we explore the impact of stochastic growth on our results, and find that it facilitates the promotion of cooperation.

II. MODEL AND METHODS

A. Spatially structured population with cycles of growth, merging, and dilution

We model spatially structured populations on a fully connected graph (or clique) with D nodes, each one comprising a well-mixed subpopulation, also known as a deme. We consider two possible types of individuals: cooperators and defectors (or cheaters). As we are interested in the emergence of cooperation, we denote cooperators by M (mutants) and defectors by W (wild-type), and their respective fitnesses by f_M and f_W. Fitnesses are understood as their maximal growth rates in the exponential phase.

In a recent study [34], we investigated the evolution of cooperation in deme-structured populations on graphs, using models we introduced in Refs. [28,29]. We assumed that demes are connected by migrations under soft selection (i.e., migrations are not affected by deme size). This gave rise to a separation of scales where cooperation had an impact only within demes, and not at the scale of the population. As a result, cooperation was not advantaged by spatial structure. Here, we extend the model of deme-structured populations on graphs from Ref. [29] to a specific case of hard selection, where migrations are proportional to the size of the deme of origin after growth, and we investigate the evolution of cooperation in this case. Specifically, the structured population undergoes three-step cycles of deterministic logistic growth with carrying capacity K within each deme, merging of all demes, and dilution and formation of new demes, as follows.

B. Growth in each deme

Starting from a bottleneck with B individuals, each deme undergoes a logistic growth phase during time t, with a carrying capacity $K \gg 1$. To describe cooperation in a minimal way, we model interactions between individuals in a deme with the prisoner's dilemma game, as in Ref. [34], and inspired by evolutionary game theory models on graphs with one individual per node [13,40]. The payoff matrix reads

$$P = \begin{pmatrix} b-c & -c \\ b & 0 \end{pmatrix}, \tag{1}$$

where $b > c > 0$. Here, b models the benefit brought by interacting with a cooperator, while c models the individual cost of cooperation for a cooperator. If a cooperator interacts with a defector, the cooperator receives a payoff $-c < 0$ whereas the cheater receives a payoff $b > c > 0$. If two cooperators interact, they both receive a payoff $b - c$. Finally, if two defectors interact, the payoff is zero.

In a well-mixed deme, each individual interacts with all other individuals. Denoting by k the number of cooperators, l the number of defectors in a deme, and $N = k + l$ the deme size, the total payoff of any individual of type M or W is

$$\begin{aligned} \pi_M(k,N) &= (b-c)\frac{k-1}{N-1} - c\frac{N-k}{N-1}, \\ \pi_W(k,N) &= b\frac{k}{N-1}. \end{aligned} \tag{2}$$

We assume that an individual's fitness depends linearly on the payoff it receives, such that the frequency-dependent fitnesses $f_M(k,N)$ for a cooperator and $f_W(k,N)$ for a defector are given by

$$\begin{aligned} f_M(k,N) &= 1 - w + w\pi_M(k,N), \\ f_W(k,N) &= 1 - w + w\pi_W(k,N), \end{aligned} \tag{3}$$

with w the intensity of selection. We interpret fitness as growth rate in the exponential phase, and focus on the weak selection regime $w \ll 1$.

For $\tau \in [0, t]$, the numbers of cooperators and defectors satisfy the following ordinary differential equations:

$$\frac{dk}{d\tau} = k f_M \left(1 - \frac{k+l}{K}\right),$$
$$\frac{dl}{d\tau} = l f_W \left(1 - \frac{k+l}{K}\right). \tag{4}$$

Rewriting Eq. (4) in terms of deme size N and of cooperator fraction $x = k/N$ leads to

$$\frac{dN}{d\tau} = [1 - w + w(b-c)x]N\left(1 - \frac{N}{K}\right),$$
$$\frac{dx}{d\tau} = -wx(1-x)\left(\frac{b}{N-1} + c\right)\left(1 - \frac{N}{K}\right). \tag{5}$$

Note that $dx/d\tau \leqslant 0$ since $b > c > 0$. Hence, in each deme, the fraction of cooperators decreases during the growth phase. Also note that the carrying capacity K does not depend on the cooperator fraction: if growth time is long enough, all demes reach the same size K.

In the weak selection regime $w \ll 1$, the solution of this system of nonlinear ordinary differential equations can be expanded as (see Ref. [41] Sec. 1.1 for details)

$$N(\tau) = \frac{K}{1 + \frac{K-B}{B}e^{-\tau}}\left(1 + w\frac{\tau[(b-c)x_0 - 1]}{1 + \frac{B}{K-B}e^{\tau}}\right) + \mathcal{O}(w^2),$$
$$x(\tau) = x_0 - wx_0(1-x_0)\Bigg[\tau(c-b) + b\ln\left(\frac{B(K-1)e^{\tau} + B - K}{K(B-1)}\right) - c\ln\left(\frac{B(e^{\tau}-1)+K}{K}\right)\Bigg] + \mathcal{O}(w^2), \tag{6}$$

where x_0 denotes the initial proportion of cooperators. While these equations hold within a deme, we also consider the overall fraction of cooperators in the structured population, denoted by $X(\tau)$, which is the average of cooperator fractions in each deme, weighted by their sizes.

C. Merging and dilution modeling hard selection

After the growth phase, we assume that all demes are merged to form one well-mixed population, and then new demes are formed by sampling from this well-mixed population, resulting in a new bottleneck state, see Fig. 1. This process was previously considered in Refs. [14,20]. Specifically, after merging, the system is brought back to a new bottleneck state of D demes, each of size B by a dilution step, where each deme is formed by sampling B individuals from the merged population. As the grown population is assumed to be large ($K \gg B$), we employ sampling with replacement. Hence, the new bottleneck state of each deme is formed by a binomial law with B trials and a probability $X' = X(t)$ of sampling a mutant.

This merging and dilution process can be viewed as a particular case of migrations with hard selection in a clique.

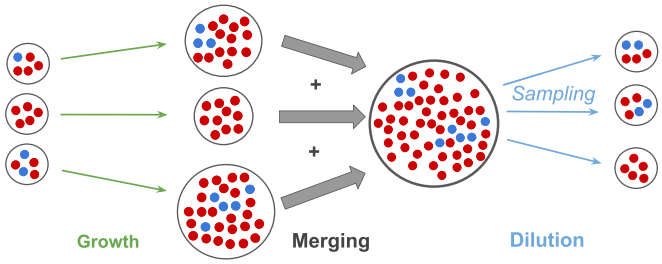


FIG. 1. Representation of one full cycle of growth-merging-dilution of the model for $D = 3$ demes. Blue markers represent cooperators, while red markers represent defectors. The initial state of the demes is shown on the left. The demes first undergo a local growth phase, followed by a merging where all individuals are put together. Then, the dilution step consists of three binomial samplings that determine the new bottleneck compositions of the three demes.

Selection is hard because each deme contributes to the next bottleneck state proportionally to its size after growth. To make the link explicit, consider a migration step on a clique graph of grown demes, followed by a local binomial sampling in each of them. In a clique, migrations occur with equal probability from one deme to another. Here, we assume that migrations from each deme to itself also have the same probability, yielding a probability $m_{ij} = 1/D$ for an individual in deme i to migrate to deme j, for all i and j. Let us denote by $N_i' = N_i(t)$ [resp. $x_i' = x_i(t)$] the size of deme i (resp. the fraction of cooperators in that deme) after the growth phase. Assuming that grown demes are large enough for all fluctuations to be neglected, during the migration step, $N_i' m_{ij} = N_i'/D$ individuals, including $N_i' x_i' m_{ij} = N_i' x_i'/D$ mutants, go from deme i to deme j. The fact that these numbers are proportional to the grown size N_i' of the deme of origin i illustrates that the process comprises hard selection. After this migration step, all demes have the same size $\sum_i N_i'/D$ and the same mutant fraction $X' = \sum_i N_i' x_i' / \sum_i N_i'$. Then, binomial sampling is performed locally in each deme to retain only B individuals per deme, with a probability X' of sampling a mutant. Note that this corresponds to the usual sampling method in structured Wright-Fisher models [42], and is one of the sampling schemes considered in Ref. [29] (under the name "local binomial").

III. RESULTS

A. Cooperation can be transiently promoted on the graph during a growth phase

We first ask whether the overall cooperator fraction can increase during a growth phase. To address this question, starting from Eq. (6), we express the excess overall cooperator fraction $\Delta X(\tau) = X(\tau) - X(0)$ in the population during growth (for $\tau \in [0, t]$); see Ref. [41] Sec. 1.2.1. We obtain, in the weak fitness intensity regime $w \ll 1$,

$$\Delta X(\tau) = w[\Delta X_a(\tau) - \Delta X_b(\tau)] + \mathcal{O}(w^2), \text{ with} \tag{7}$$

$$\Delta X_a(\tau) = \mathrm{Var}(x_i)\frac{\tau(b-c)}{1 + \frac{B}{K-B}e^{\tau}}, \text{ and} \tag{8}$$

$$\Delta X_b(\tau) = \langle x_i(1-x_i)\rangle \Bigg[\tau(c-b) + b \ln\left(\frac{B(K-1)e^{\tau} + B - K}{K(B-1)}\right) - c \ln\left(\frac{B(e^{\tau}-1)+K}{K}\right)\Bigg], \tag{9}$$

where x_i denotes the initial fraction of cooperators in deme i, for $1 \leqslant i \leqslant D$. Here, averages over demes are denoted by $\langle . \rangle = (1/D)\sum_i (.)$, and the variance in the initial cooperator fraction across demes is $\mathrm{Var}(x_i) = \langle x_i^2 \rangle - \langle x_i \rangle^2$. To first order in w, Eq. (7) is a multilevel Price equation [38,39,43–45] (see Ref. [41] Sec. 1.2.4 for details), which involves a trade-off between two terms:

(1) $\Delta X_a(\tau) \geqslant 0$ corresponds to between-deme selection. Cooperators bring a collective benefit to a deme's growth, and demes that start with more cooperators grow faster, thereby yielding a larger contribution to the overall cooperator fraction. The greater the heterogeneity in the initial deme compositions, the stronger this effect is.

(2) $-\Delta X_b(\tau)$ corresponds to within-deme selection. It satisfies $-\Delta X_b(\tau) \leqslant 0$, see Ref. [41] Sec. 1.2.2. Qualitatively, this is because cooperators are disadvantaged within each deme due to the cost of cooperation, and have a lower fitness than cheaters (see Model and Methods), yielding a decrease in the cooperator fraction in each deme.

The overall cooperator fraction grows if $\Delta X(\tau) > 0$, i.e., if the global benefit of cooperation is greater than the local cost, that is $\Delta X_a(\tau) > \Delta X_b(\tau)$.

Figure 2 shows a situation where $\Delta X(\tau) > 0$ transiently, while $x_i(\tau)$ decreases in each deme i [e.g., in deme 1, see Fig. 2(a)]. We further observe that our analytical approximations in Eq. (6) and Eq. (7) agree well with numerical results in the weak selection regime.

Figure 2(b) further shows the time evolution of ΔX_a and ΔX_b. We observe that the between-group selection term ΔX_a transiently exceeds the within-group term ΔX_b, leading to $\Delta X(\tau) > 0$. Later, ΔX_a decreases and tends to zero as deme size tends to their carrying capacity K [see Fig. 2(a)], and the size contrast between demes vanishes. We then have $\Delta X(\tau) < 0$. In this model, if there is sufficient heterogeneity in the initial cooperator fractions across different demes, and if demes have not reached saturation by the end of the growth phase, then the resulting contrast in deme sizes can yield $\Delta X(\tau) > 0$. This situation is known as Simpson's paradox: global cooperator fraction increases even though local cooperator fraction decreases in each deme, i.e., $\Delta x_i(\tau) = x_i(\tau) - x_i(0) < 0$ for all i. Such an effect was previously described in experiments and in modeling studies [6,14–17,20–22]. In particular, models with cycles of growth, merging, and dilution were investigated in Refs. [6,14–17]. While the advantage of cooperation was investigated in these previous studies, our analytical resolution of the dynamics in the weak selection regime allows us to analytically predict the transient advantage of cooperation and to quantitatively interpret it as a trade-off between intrademe and interdeme dynamics. The transient nature of the benefit of cooperation is due to growth saturation. Indeed, in Ref. [41] Sec. 2.1, we consider

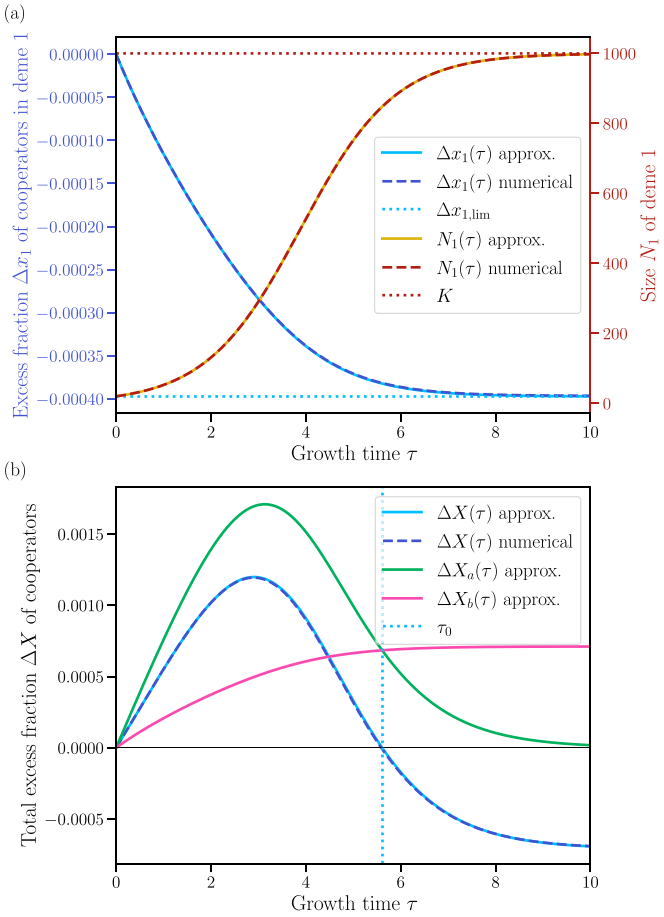


FIG. 2. Growth phase: evolution of the fraction of cooperators in a deme and in the population. (a) Excess fraction $\Delta x_1(\tau) = x_1(\tau) - x_1(0)$ of cooperators in one deme, namely, deme 1, and size N_1 of this deme, versus growth time τ. We show the numerical solution of Eq. (5) and the analytical approximation of Eq. (6), obtained in the weak selection regime. We indicate the long-time asymptotic value $\Delta x_{1,\mathrm{lim}}$ of Δx_1, obtained from Eq. (6), and the carrying capacity K (horizontal dotted lines). (b) Excess fraction $\Delta X(\tau) = X(\tau) - X(0)$ of cooperators in the total population versus growth time τ. As in panel (a), we show the numerical solution and the analytical approximation, here given by Eq. (7). In addition, we show the two terms from Eqs. (8) and (9) into which $\Delta X(\tau)$ can be decomposed. We also show the largest time $\tau_0 > 0$ such that $\Delta X(\tau) \geqslant 0$ (vertical dotted line). In both panels, results are obtained for a population of $D = 5$ demes, each with initial size $B = 20$ and carrying capacity $K = 1000$, using initial compositions $x_1(\tau = 0) = 1/10$, $x_2(0) = 1/4$, $x_3(0) = 1/2$, $x_4(0) = 3/4$ and $x_5(0) = 9/10$, fitness intensity $w = 10^{-3}$, benefit $b = 10$, and cost $c = 1$.

the case of continued exponential growth. In that case, when cooperation is promoted during growth at the scale of the full population, the effect increases over time, because the difference between the sizes of demes with a larger and a smaller fraction of cooperators keeps increasing. Note that in the presence of growth saturation, if the carrying capacity increases with the cooperator fraction, the benefit of cooperation can increase for longer growth times [14–17,19]. Here, for the sake of simplicity, we have assumed that K does not depend on population composition.

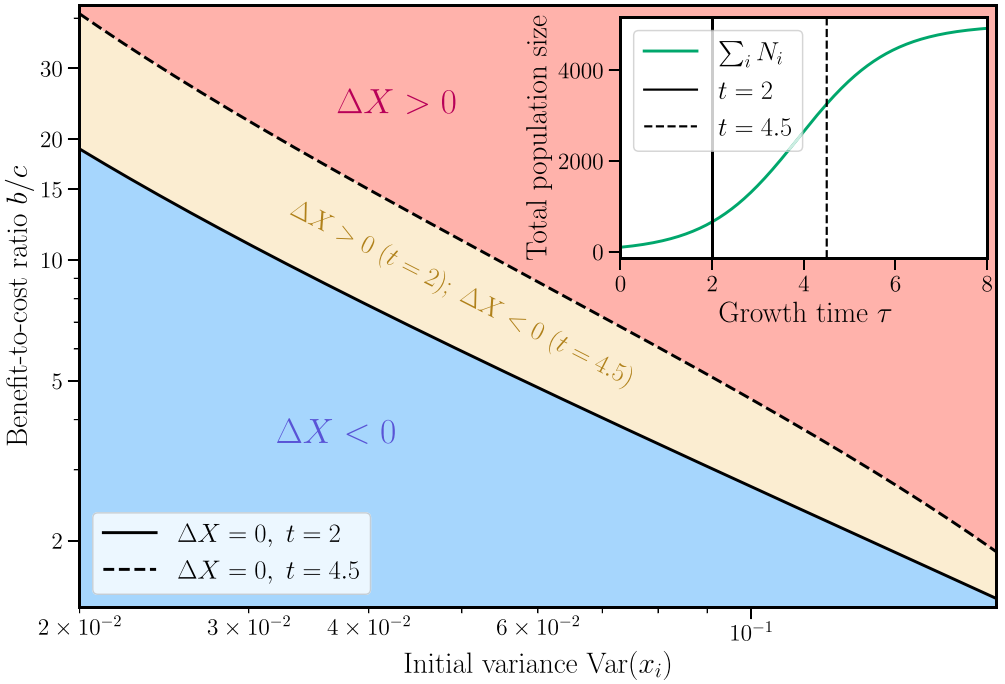


FIG. 3. Impact of the benefit-to-cost ratio and of the variance in deme compositions on the evolution of cooperator fraction during growth. We show a phase diagram, representing whether $\Delta X > 0$ or $\Delta X < 0$, as a function of the benefit-to-cost ratio b/c and the variance $\mathrm{Var}(x_i)$ of the initial deme compositions, for two different durations of the growth phase. The separation between zones, namely, $\Delta X = 0$, is given by Eq. (18) of Ref. [41]. Results are obtained for a population of $D = 5$ demes, each with initial size $B = 20$ and carrying capacity $K = 1000$, using different initial compositions with mean $\langle x_i \rangle = 0.5$, fitness intensity $w = 10^{-3}$, cost $c = 1$, and growth phase durations $t = 2$ and $t = 4.5$. The inset shows the analytical approximation for the total population size $\sum_{i=1}^{D} N_i$ versus growth time τ, using Eq. (6) and the same parameter values, for $b = 10$.

For a given growth time t and for given initial deme compositions, Eq. (7) can be used to compute the threshold value of the benefit-to-cost ratio b/c beyond which cooperation is promoted in the structured population during growth; see Ref. [41] Sec. 1.2.3. The smaller the variance in the initial deme compositions, the larger b/c must be for cooperation to be favored during growth; see Fig. 3. Assuming that the variance in the initial deme compositions is large enough and the growth time not too short, one can show that this threshold value of b/c increases with time (matching the two cases shown in Fig. 3), and that cooperation becomes impossible beyond a certain growth time; see Ref. [41] Sec. 1.2.3. Qualitatively, this is because of the saturation of demes, as the carrying capacity K is here assumed to be independent of cooperator fraction, which entails that cooperator-rich demes lose their advantage of being larger as saturation is reached.

B. An effective fitness parameter determines if cooperation is favored on average under cycles of dilution-growth-merging

So far, we determined the conditions that favor cooperation during a given deterministic growth phase. Let us now consider a full cycle of dilution-growth-merging, which involves a stochastic dilution step via binomial sampling, and ask whether cooperation is advantaged on average during such a cycle. For this, we consider the expectation value under the binomial law used for sampling of the difference $\Delta X' = X'_n - X'_{n-1}$ in overall cooperator fraction, taken between the end of the growth phase of one cycle (say cycle $n-1$) and the end of the growth phase of the next one (n). It can be expressed as (see Ref. [41] Sec. 1.3 for details)

$$\mathbb{E}[\Delta X'] = w s(t) X'_{n-1}(1 - X'_{n-1}) + \mathcal{O}(w^2), \tag{10}$$

where $s(t)$ is an effective fitness that depends on time and on model parameters:

$$s(t) = \frac{D-1}{DB} \frac{t(b-c)}{1 + \frac{B}{K-B} e^t} - \frac{B-1}{B} \Bigg[t(c-b) + b \ln\left(\frac{B(K-1)e^t + B - K}{K(B-1)} \right) - c \ln\left(\frac{B(e^t - 1) + K}{K} \right) \Bigg]. \tag{11}$$

The effective fitness $s(t)$ features an interplay between between-deme selection [first term, nonnegative, coming from the expectation of ΔX_a in Eq. (7)] and within-deme selection [second term, nonpositive, coming from the expectation of $-\Delta X_b$ in Eq. (7)]. Equation (10) shows that, assuming $0 < X'_{n-1} < 1$, cooperation is favored on average over one cycle of dilution-growth-merging (i.e., $\mathbb{E}[\Delta X'] > 0$) if and only if

$$s(t) > 0. \tag{12}$$

For brevity, we henceforth omit the explicit time dependence of s. For s to be positive, the dilution step needs to generate

enough variance in the initial deme compositions to yield a Simpson's paradox scenario during the subsequent growth phase. For this, it is important that the bottleneck size B is small enough, as the expectation value of the variance of deme compositions just after dilution is inversely proportional to B (see Ref. [41] Sec. 1.3). While this point was previously highlighted [6,14–17,20,21], here we provide an analytical condition for cooperation to be favored on average under cycles of dilution-growth-merging. Note that it can be expressed as a threshold value of the benefit-to-cost ratio b/c beyond which cooperation is favored; see Ref. [41] Sec. 1.3.2. Studying s also allows us to investigate extreme parameter regimes; see Ref. [41] Sec. 2.2. In particular, for large growth times, all demes saturate at the carrying capacity and cooperation cannot be promoted. Conversely, in the limit of large carrying capacities, the promotion of cooperation is not transient but increases, as exponential growth continues. Finally, for large bottleneck sizes, cooperation cannot be promoted, because small bottlenecks are needed to obtain contrast across demes after the dilution step.

While we derived Eq. (12) by focusing on one cycle, this condition does not depend on the precise cycle considered (e.g., on the initial cooperator proportions in each deme at the beginning of it). Hence, it is a general condition, valid for any cycle throughout the dynamics and for any number of cycles. In our model, cooperation can be favored in a clique-structured population with weak selection, under repeated cycles of dilution, logistic growth and merging, if and only if Eq. (12) is satisfied. Hard selection, implemented here by merging and dilution, plays a fundamental role, as it allows the promotion of the collective benefit of cooperation. Indeed, it is via this mechanism that larger demes contribute more to the next bottleneck state. Furthermore, the benefit of cooperation is maintained across cycles through stringent dilution events that yield large compositional variance between demes at each bottleneck.

C. Analytical calculation of the fixation probability of cooperator mutants under weak selection

If cooperation appears through a mutation, it will first be present in a single individual, whose lineage will thus initially be subject to strong finite-size fluctuations (known as genetic drift). In the present model, where growth is deterministic, stochasticity arises from the dilution step, which is modeled by binomial sampling. What is the probability that cooperators ultimately take over the whole population, starting from any initial population composition, e.g., from a single cooperator mutant? To address this question, we need to go beyond averaged dynamics and to perform a stochastic treatment of the system under successive cycles of growth, merging, and dilution. A challenge is that we cannot assume that deme sizes are large, given that small bottlenecks and strong variance are necessary for cooperation to be favored on average. This precludes the use of the branching process approximation [29,46,47] or of the diffusion approximation [48] at the scale of demes, since they both require $B \gg 1$ to hold. Hence, we perform a calculation of the fixation probability in the weak selection regime $w \ll 1$, without making any assumption on B.

Let us denote by i_k the initial number of cooperators in each deme $k \in \{1, \dots, D\}$ at a bottleneck, and introduce $\boldsymbol{i} = (i_1, \dots, i_D)$. Our goal is to determine the fixation probability $p_{\boldsymbol{i}}$ of cooperators starting from any initial population composition $\boldsymbol{i}$. We have $p_{(0,\dots,0)} = 0$ and $p_{(B,\dots,B)} = 1$. Let $P_{\boldsymbol{i}\to\boldsymbol{j}}$ be the probability of sampling $\boldsymbol{j} = (j_1, \dots, j_D)$ cooperators to form each deme's new bottleneck upon a dilution step, after growth and merging, if the previous bottleneck had $\boldsymbol{i} = (i_1, \dots, i_D)$ cooperators. Since the dilution step is assumed to proceed through independent binomial samplings (i.e., with replacement), we have

$$P_{\boldsymbol{i}\to\boldsymbol{j}} = \prod_{k=1}^{D} \binom{B}{j_k} (X')^{j_k} (1 - X')^{B - j_k}, \tag{13}$$

where $X' = X + \Delta X$ denotes the overall cooperator fraction at the end of growth, with $X = \sum_{k=1}^{D} i_k/(DB)$ the overall initial cooperator fraction before growth and $\Delta X = \Delta X(t)$ given by Eq. (7) with $\tau = t$. For this Markov chain, the fixation probability $p_{\boldsymbol{i}}$ is the probability of eventually reaching the absorbing state $(B, \dots, B)$ from the initial configuration $\boldsymbol{i}$. Considering all possible states after the first step of the Markov chain, we can write a recurrence relation on $p_{\boldsymbol{i}}$ (which is the discrete analog of a steady-state Kolmogorov backward equation):

$$p_{\boldsymbol{i}} = \sum_{j_1=0,\dots,j_D=0}^{B} P_{\boldsymbol{i}\to\boldsymbol{j}} p_{\boldsymbol{j}}. \tag{14}$$

Performing a first-order expansion of Eq. (14) in the weak selection regime (see Ref. [41] Sec. 1.4 for details), we obtain the following expression for the fixation probability:

$$p_{\boldsymbol{i}} = X + \Delta X + wsDBX(1 - X) + \mathcal{O}(w^2), \tag{15}$$

where $\Delta X = \Delta X(t) = \mathcal{O}(w)$ is given by Eq. (7) and characterizes the evolution of the cooperator fraction during the first growth phase, while s is the effective fitness parameter defined in Eq. (11) and characterizes the cycles of dilution-growth-merging. Note that the fixation probability of defectors, written in terms of the fraction of defectors $Y = 1 - X$, takes the same form as the one of cooperators in Eq. (15), but with the opposite effective fitness coefficient; see Ref. [41] Sec. 1.4.1. Equation (15) is an analytical formula that holds for any initial population composition $\boldsymbol{i}$ in a spatially structured population undergoing cycles of logistic growth, merging, and dilution, in the weak selection regime. It shows that whether cooperation is more or less likely to take over depends on the first growth phase, via ΔX, and on the subsequent cycles of dilution-growth-merging, via s, in addition to the initial composition, via X. Importantly, the result in Eq. (15) holds for small bottleneck sizes, contrary to results obtained using branching process or diffusion approximations. Note that our weak selection assumption requires $wDB \ll 1$, which entails that the domain of validity of Eq. (15) is different from that of a branching process approximation (which, for fitness intensity w and population size DB, assumes $1/(DB) \ll w \ll 1$ and $DB \gg 1$) or of a diffusion approximation [which assumes $w \sim 1/(DB)$ and $DB \gg 1$].

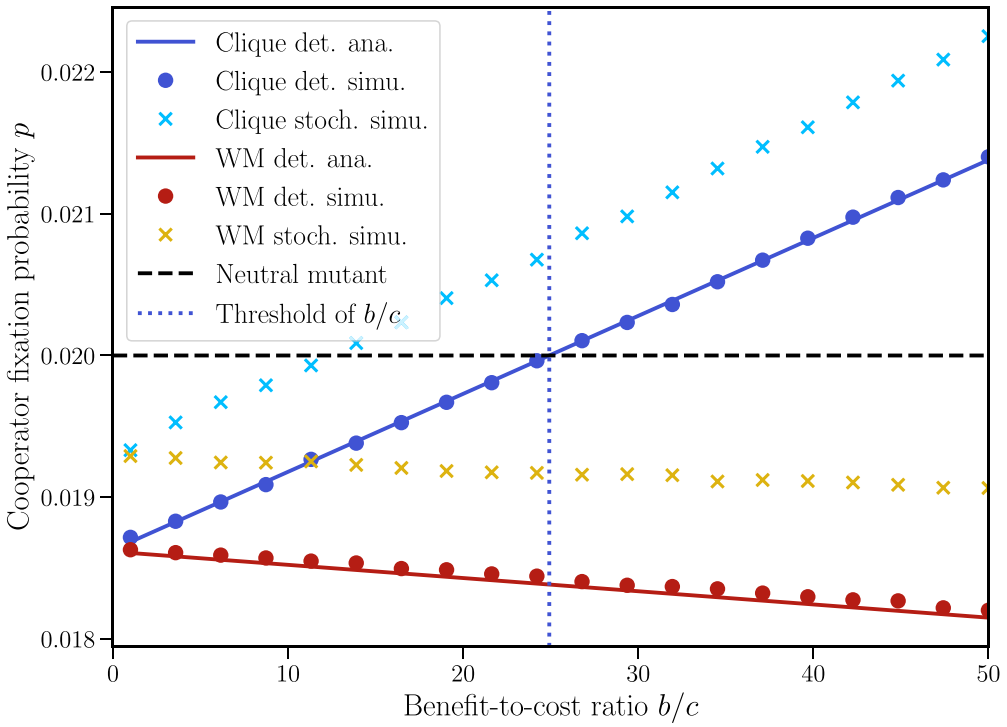


FIG. 4. Fixation of cooperation. We show the fixation probability p of cooperation, starting from a single cooperator in the whole population, versus the benefit-to-cost ratio b/c, both for our structured population and for a well-mixed ("WM") population with the same total bottleneck size DB and carrying capacity DK. Round markers: numerical simulation ("simu.") results with deterministic growth ("det."); solid lines: corresponding analytical predictions ("ana.") from Eq. (15). The threshold of b/c beyond which cooperator fixation is predicted to be promoted (with deterministic growth), given by Eq. (63) of Ref. [41], is shown as a vertical dotted blue line. Cross markers: numerical simulation results with stochastic growth ("stoch."). The fixation probability of a neutral mutant, $p = 1/(DB)$, is shown for reference (horizontal dashed line). Parameter values are $D = 5$, $B = 10$, $K = 1000$ for a structured population; $D = 1$, $B = 50$, $K = 5000$ for a well-mixed population; for both, $t = 3$, $w = 5 \times 10^{-4}$ and $c = 1$. Simulation results are obtained over $N = 10^8$ realizations.

D. Cooperator fixation can be favored by spatial structure with merging dynamics

Let us consider as reference neutral mutants, i.e., mutants with no fitness difference from the wild-type at any frequency, and let us compare cooperators to this baseline. The fixation probability of cooperators is greater than that of neutral mutants starting from the same initial proportions if $p_i > X$. Using Eq. (15), this condition can be expressed as $\Delta X + wsDBX(1-X) > 0$. It allows us to predict the threshold value of the benefit-to-cost ratio b/c beyond which cooperator fixation is promoted in our spatially structured population; see Ref. [41] Sec. 1.4.2.

Figure 4 shows a comparison between our analytical expression of the fixation probability in Eq. (15) and numerical simulation results, starting from a single cooperator mutant. For this, we performed exact stochastic simulations of our model (with cycles of deterministic growth, merging, and dilution via binomial sampling), and estimated p_i as the proportion of simulations (all starting from $\boldsymbol{i}$) that reach the absorbing state $X = 1$ (as opposed to the other absorbing state $X = 0$). We obtain very good agreement between analytical and numerical results. We observe that, as the benefit-to-cost ratio b/c increases, the fixation probability of a cooperator increases as well. When b/c reaches the predicted threshold value, the fixation probability of a cooperator becomes larger than that of a neutral mutant. This stands in strong contrast with a well-mixed population of the same size (also shown in Fig. 4), where a cooperator is never more likely to fix than a neutral mutant, because of the cost of cooperation. Here, cooperation is promoted by the spatial structure considered, and our analytical calculations allow us to determine when and how much this happens, provided that selection is weak.

E. Stochastic growth further enhances the promotion of cooperation

In our analysis, we have assumed deterministic logistic growth. We showed that for cooperation to be maintained, the bottleneck size B needs to be small enough for the dilution step to maintain a high variance in deme compositions. Given these small bottleneck sizes, stochastic effects associated with demographic fluctuations during the growth phase can in fact have an important impact. How do our conclusions change if the growth phase is stochastic? To address this question, we consider that each individual can divide at a given rate, matching the one used in our deterministic growth model. We perform simulations of this stochastic growth phase using a Gillespie algorithm; see Ref. [41] Sec. 3 for details. The merging and dilution steps are unchanged. Note that this modified model comprises two sources of stochasticity, namely, the dilution process and the growth process.

In Fig. 4, we compare the fixation probability results in simulations using deterministic and stochastic growth. We find that the fixation probability of a cooperator mutant is higher with stochastic growth than with deterministic growth. Hence, demographic fluctuations during growth can further enhance the promotion of cooperation. As previously noted in Ref. [14], this is because fluctuations are amplified asymmetrically in this model, in the sense that growth is enhanced if an additional cooperator appears due to a division, but hindered if an additional cheater appears. Our simulation results further suggest that the analytical conditions we derived with deterministic growth provide sufficient conditions for cooperation to be promoted, even with stochastic growth.

IV. DISCUSSION

In this work, we considered a minimal model for the evolution of cooperation in deme-structured populations under hard selection. Cooperative interactions were modeled by the prisoner's dilemma, and hard selection by dilution-growth-merging cycles, where each deme contributes to the next bottleneck state in proportion to its size after a phase of local growth. We initially assumed deterministic local growth, but we described dilution via stochastic sampling, and we assumed weak selection. We analytically determined the time evolution of the cooperator fraction during logistic growth, and interpreted this result as a multilevel Price equation, highlighting a trade-off between within-deme dynamics, where cooperators are disadvantaged, and between-deme dynamics, where demes with more cooperators are advantaged. We then analyzed dilution-growth-merging cycles and derived an analytical condition for the cooperator fraction to increase on average under that dynamics. This requires small bottleneck deme sizes, which generate sufficient variance in deme composition for cooperation to be favored in the whole structured population. Next, we analytically expressed the fixation probability of cooperators under weak selection, without assuming large demes. This yielded a criterion for cooperators to have a higher fixation probability than neutral mutants, and hence for cooperation to be advantaged by natural selection in the spatially structured population. Finally, numerical simulations showed that stochastic growth further promotes cooperation.

A key insight is that, in our simple model of cooperation in deme-structured populations, the mode of selection is decisive: while cooperation cannot be favored under soft selection [34], the present study shows that it can be favored under hard selection. Here, we implemented hard selection through the dilution-growth-merging process [16,17], whereby demes contribute to the next bottleneck state in proportion to their sizes after growth. As a result, demes with a higher fraction of cooperators can contribute more to the next bottleneck, thanks to their growth advantage. This growth advantage is transient under logistic growth but permanent under continued exponential growth. This coupling between the dynamics of population size and composition has been highlighted previously in Refs. [14–17,20–22]. Our study connects these results with those of models on graphs with a single individual per node, where spatial structure can favor cooperation under certain individual-level update rules [12,13].

Our work opens several perspectives for further theoretical analysis. First, for simplicity, we assumed that the carrying capacity of a deme is independent of its cooperator fraction. However, a higher cooperator fraction can be associated with a larger carrying capacity [14–17,20], which enhances the transient advantage of cooperation during logistic growth, and introduces an additional mechanism by which spatial structure can promote cooperation, namely, group fixation: demes where cooperators have fixed then become larger than other demes [16]. Extending our analytical calculations to this case would therefore be of interest. Second, we assumed deterministic growth in most of our analysis, but we observed numerically that stochastic growth can enhance the fixation of cooperators. Further analytical insight into this aspect could be obtained using a van Kampen expansion, as in Refs. [14–17]. A challenge, however, is that this approach relies on an expansion in large system sizes, whereas the promotion of cooperation necessitates small bottleneck sizes. Moreover, while valuable insight was obtained in Refs. [14–17] by focusing on the early stages of growth, analytically determining conditions for cooperation to be promoted would likely require considering the full growth phase. More generally, stochastic growth could be incorporated using stochastic differential equations, but existing work generally focuses on the large-population regime [49]. Third, our analytical expression of the fixation probability assumes weak selection but remains valid for small bottleneck sizes. Thus, a promising direction for future work is to extend our analysis beyond the weak selection regime. Besides, the domain of validity of our current approach differs from that of diffusion and branching process approximations, which assume large deme sizes, and more general descriptions encompassing these different regimes would be highly interesting in dilution-growth models and in Wright-Fisher, which are closely related [29], as well as in models with partial updates, which bridge Wright-Fisher and Moran models [50].

More generally, while the merging process facilitates analytical progress thanks to its strong symmetries, it would be interesting to study other forms of hard selection in more complex population structures. First, one could consider a clique where each deme contributes in proportion to its productivity (i.e., its size after growth), but where the probability that an organism migrates to another deme differs from the probability that it stays in its deme of origin (thus going beyond the specific case of merging). Next, one could consider more general graphs, in order to establish a more complete link with results from evolutionary graph theory [12,13]. Studying other forms of cooperative interactions is also a promising direction and would allow closer links to specific natural or experimental systems. This includes considering games other than the prisoner's dilemma, such as the snowdrift game [51], modeling cooperative antibiotic resistance [52–55], and explicitly describing the dynamics of diffusible public goods [7,56–58] and resource limitation [59].

ACKNOWLEDGMENTS

This project has received funding from the European Research Council (ERC) under the European Union's Horizon

2020 Research and Innovation Program (Grant Agreement No. 851173 to A.-F. B.).

DATA AVAILABILITY

Our code is freely available at [60].

[1] R. Axelrod and W. D. Hamilton, The evolution of cooperation, Science **211**, 1390 (1981).

[2] N. S. Wingreen and S. A. Levin, Cooperation among microorganisms, PLoS Biol. **4**, e299 (2006).

[3] H. Celiker and J. Gore, Cellular cooperation: Insights from microbes, Trends Cell Biol. **23**, 9 (2013).

[4] L. A. Dugatkin, *Cooperation Among Animals: An Evolutionary Perspective* (Oxford University Press, USA, 1997).

[5] I. D. Chase, Cooperative and noncooperative behavior in animals, Am. Nat. **115**, 827 (1980).

[6] J. Cremer, A. Melbinger, K. Wienand, T. Henriquez, H. Jung, and E. Frey, Cooperation in microbial populations: Theory and experimental model systems, J. Mol. Biol. **431**, 4599 (2019).

[7] D. B. Borenstein, Y. Meir, J. W. Shaevitz, and N. S. Wingreen, Non-local interaction via diffusible resource prevents coexistence of cooperators and cheaters in a lattice model, PLoS One **8**, e63304 (2013).

[8] W. D. Hamilton, The genetical evolution of social behaviour I, J. Theor. Biol. **7**, 1 (1964).

[9] W. D. Hamilton, The genetical evolution of social behaviour II, J. Theor. Biol. **7**, 17 (1964).

[10] A. S. Griffin, S. A. West, and A. Buckling, Cooperation and competition in pathogenic bacteria, Nature (London) **430**, 1024 (2004).

[11] L. J. Belcher, A. E. Dewar, M. Ghoul, and S. A. West, Kin selection for cooperation in natural bacterial populations, Proc. Natl. Acad. Sci. USA **119**, e2119070119 (2022).

[12] H. Ohtsuki and M. A. Nowak, Evolutionary games on cycles, Proc. R. Soc. Ser. B **273**, 2249 (2006).

[13] H. Ohtsuki, C. Hauert, E. Lieberman, and M. A. Nowak, A simple rule for the evolution of cooperation on graphs and social networks, Nature (London) **441**, 502 (2006).

[14] A. Melbinger, J. Cremer, and E. Frey, Evolutionary game theory in growing populations, Phys. Rev. Lett. **105**, 178101 (2010).

[15] J. Cremer, A. Melbinger, and E. Frey, Evolutionary and population dynamics: A coupled approach, Phys. Rev. E **84**, 051921 (2011).

[16] J. Cremer, A. Melbinger, and E. Frey, Growth dynamics and the evolution of cooperation in microbial populations, Sci. Rep. **2**, 281 (2012).

[17] A. Melbinger, J. Cremer, and E. Frey, The emergence of cooperation from a single mutant during microbial life cycles, J. R. Soc. Interface **12**, 20150171 (2015).

[18] P. Czuppon and P. Pfaffelhuber, A spatial model for selection and cooperation, J. Appl. Probab. **54**, 522 (2017).

[19] J. J. Arenzon and L. Peliti, Emergent cooperative behavior in transient compartments, Phys. Rev. E **108**, 034409 (2023).

[20] J. S. Chuang, O. Rivoire, and S. Leibler, Simpson's paradox in a synthetic microbial system, Science **323**, 272 (2009).

[21] J. S. Chuang, O. Rivoire, and S. Leibler, Cooperation and Hamilton's rule in a simple synthetic microbial system, Mol. Syst. Biol. **6**, MSB201057 (2010).

[22] F. Becker, K. Wienand, M. Lechner, E. Frey, and H. Jung, Interactions mediated by a public good transiently increase cooperativity in growing *Pseudomonas putida* metapopulations, Sci. Rep. **8**, 4093 (2018).

[23] T. Kay, L. Keller, and L. Lehmann, The evolution of altruism and the serial rediscovery of the role of relatedness, Proc. Natl. Acad. Sci. USA **117**, 28894 (2020).

[24] P. E. Turner and L. Chao, Prisoner's dilemma in an RNA virus, Nature (London) **398**, 441 (1999).

[25] M. Doebeli and C. Hauert, Models of cooperation based on the prisoner's dilemma and the snowdrift game, Ecol. Lett. **8**, 748 (2005).

[26] C. S. Gokhale and A. Traulsen, Evolutionary multiplayer games, Dyn. Games Appl. **4**, 468 (2014).

[27] E. Lieberman, C. Hauert, and M. A. Nowak, Evolutionary dynamics on graphs, Nature (London) **433**, 312 (2005).

[28] L. Marrec, I. Lamberti, and A.-F. Bitbol, Toward a universal model for spatially structured populations, Phys. Rev. Lett. **127**, 218102 (2021).

[29] A. Abbara and A.-F. Bitbol, Frequent asymmetric migrations suppress natural selection in spatially structured populations, PNAS Nexus **2**, pgad392 (2023).

[30] B. Houchmandzadeh and M. Vallade, The fixation probability of a beneficial mutation in a geographically structured population, New J. Phys. **13**, 073020 (2011).

[31] S. Yagoobi and A. Traulsen, Fixation probabilities in network structured meta-populations, Sci. Rep. **11**, 17979 (2021).

[32] S. Yagoobi, N. Sharma, and A. Traulsen, Categorizing update mechanisms for graph-structured metapopulations, J. R. Soc. Interface **20**, 20220769 (2023).

[33] P. P. Chakraborty, L. R. Nemzer, and R. Kassen, Experimental evidence that network topology can accelerate the spread of beneficial mutations, Evol. Lett. **7**, 447 (2023).

[34] A. Moawad, A. Abbara, and A.-F. Bitbol, Evolution of cooperation in deme-structured populations on graphs, Phys. Rev. E **109**, 024307 (2024).

[35] B. Wallace, Hard and soft selection revisited, Evolution **29**, 465 (1975).

[36] F. B. Christiansen, Hard and soft selection in a subdivided population, Am. Nat. **109**, 11 (1975).

[37] V. Ravigné, U. Dieckmann, and I. Olivieri, Live where you thrive: Joint evolution of habitat choice and local adaptation facilitates specialization and promotes diversity, Am. Nat. **174**, E141 (2009).

[38] G. R. Price, Extension of covariance selection mathematics, Ann. Hum. Genet. **35**, 485 (1972).

[39] C. Jeler, Price's hierarchical equation and the notion of group fitness, in *Multilevel Selection and the Theory of Evolution: Historical and Conceptual Issues* (Springer Nature, Cham, 2018), pp. 101–121.

[40] H. Ohtsuki and M. A. Nowak, The replicator equation on graphs, J. Theor. Biol. **243**, 86 (2006).

[41] See Supplemental Material http://link.aps.org/supplemental/10.1103/wlyc-rtgs for detailed derivations and additional analyses, which also includes Refs. [61–63].

[42] C. J. Burden and R. C. Griffiths, Stationary distribution of a 2-island 2-allele Wright–Fisher diffusion model with slow mutation and migration rates, Theor. Popul. Biol. **124**, 70 (2018).
[43] J. Lehtonen, The Price equation and the unity of social evolution theory, Philos. Trans. R. Soc. B **375**, 20190362 (2020).
[44] A. Gardner, Price's equation made clear, Philos. Trans. R. Soc. B **375**, 20190361 (2020).
[45] S. Okasha, *Evolution and the Levels of Selection* (Oxford University Press, New York, 2006).
[46] J. B. S. Haldane, A mathematical theory of natural and artificial selection, part V: Selection and mutation, Math. Proc. Cambridge Philos. Soc. **23**, 838 (1927).
[47] T. E. Harris, *The Theory of Branching Processes* (Springer, Berlin, 1963).
[48] M. Kimura, Diffusion models in population genetics, J. Appl. Probab. **1**, 177 (1964).
[49] A. S. Bhat and V. Guttal, Eco-evolutionary dynamics for finite populations and the noise-induced reversal of selection, Am. Nat. **205**, 1 (2025).
[50] A. Alexandre, A. Abbara, C. Fruet, C. Loverdo, and A.-F. Bitbol, Bridging Wright–Fisher and Moran models, J. Theor. Biol. **599**, 112030 (2025).
[51] J. Gore, H. Youk, and A. van Oudenaarden, Snowdrift game dynamics and facultative cheating in yeast, Nature (London) **459**, 253 (2009).
[52] L. Hernández-Navarro, M. Asker, A. M. Rucklidge, and M. Mobilia, Coupled environmental and demographic fluctuations shape the evolution of cooperative antimicrobial resistance, J. R. Soc. Interface **20**, 20230393 (2023).
[53] L. Hernández-Navarro, M. Asker, and M. Mobilia, Eco-evolutionary dynamics of cooperative antimicrobial resistance in a population of fluctuating volume and size, J. Phys. A: Math. Theor. **57**, 265003 (2024).
[54] L. Hernández-Navarro, K. Distefano, U. C. Täuber, and M. Mobilia, Slow spatial migration can help eradicate cooperative antimicrobial resistance in time-varying environments, PLoS Comput Biol **22**, e1013997 (2026).
[55] M. K. Denk-Lobnig and K. B. Wood, Spatial population dynamics of bacterial colonies with social antibiotic resistance, Proc. Natl. Acad. Sci. USA **122**, e2417065122 (2025).
[56] B. Allen, J. Gore, and M. A. Nowak, Spatial dilemmas of diffusible public goods, eLife **2**, e01169 (2013).
[57] R. Menon and K. S. Korolev, Public good diffusion limits microbial mutualism, Phys. Rev. Lett. **114**, 168102 (2015).
[58] R. Matsuzawa and J. Tanimoto, A social dilemma structure in diffusible public goods, Europhys. Lett. **116**, 38005 (2016).
[59] A. J. Waite, C. Cannistra, and W. Shou, Defectors can create conditions that rescue cooperation, PLoS Comput. Biol. **11**, e1004645 (2015).
[60] https://github.com/Bitbol-Lab/Cooperation_Merging.
[61] B. Wu, C. S. Gokhale, M. van Veelen, L. Wang, and A. Traulsen, Interpretations arising from Wrightian and Malthusian fitness under strong frequency dependent selection, Ecol. Evol. **3**, 1276 (2013).
[62] D. T. Gillespie, A general method for numerically simulating the stochastic time evolution of coupled chemical reactions, J. Comput. Phys. **22**, 403 (1976).
[63] D. T. Gillespie, Exact stochastic simulation of coupled chemical reactions, J. Phys. Chem. **81**, 2340 (1977).